Blended Cements with Limestone Filler and Kaolinitic Calcined Clay: Filler and Pozzolanic Effects

Alejandra Tironi, Ph.D.[1]; Alberto N. Scian, Ph.D.[2]; and Edgardo F. Irassar, C.Eng.[3]

Abstract: In this paper, binary and ternary blended cements (BC) based on calcined clay (CC, 0–30%) obtained from low-grade kaolinitic clay and limestone filler (LF, 0–10%) were developed and the interaction between the filler effect and pozzolanic effect on the compressive strength, hydration phases, and pore-size distribution were studied. Results show that early compressive strength decreases for high levels of replacement (10LF30CC) because of a dilution effect that cannot be compensated for by the filler and pozzolanic effects. Based on calcium hydroxide (CH) content, the addition of limestone filler in ternary blended cements is favorable to the development of pozzolanic reaction of calcined clay at an early age. This study shows that dilution, filler, and pozzolanic effects are relevant at 2 days, filler and pozzolanic effects are important at 7 days, and the pozzolanic effect is the most important at a later age. **DOI: 10.1061/(ASCE)MT.1943-5533.0001965.**

Author keywords: Kaolinitic calcined clay; Blended cement; Hydration; Pore-size distribution; Mechanical properties.

Introduction

Cement is an indispensable civil engineering material to meet modern society's needs for infrastructure, industry, and housing. Today, the cement and concrete industry promotes the reduction of CO_2 emissions and energy consumption in their processes. Among these initiatives, one is to increase the replacement percentage of supplementary cementing materials (SCM) in blended cements with similar or better performance than that traditional portland cement (Damtoft et al. 2008; Radlinski et al. 2011). SCM include fly ash, slags, and natural pozzolans (Hicks 2010; Scrivener 2014; Gedam et al. 2015). Pozzolans react chemically with calcium hydroxide to produce compounds with cementing properties. There are extensive reserves of natural pozzolans worldwide, but they generally have a fairly low reactivity and their characteristics are very variable from place to place. Calcined clays appear as a promising SCM to reach the industrýs goals (Juenger and Siddique 2015).

When kaolinitic clays are calcined between 500 and 800°C, metakaolinite (MK) is obtained. It is an amorphous reactive phase that allows the use of kaolinitic calcined clays as pozzolans (Shvarzman et al. 2003; Potgieter-Vermaak and Potgieter 2006; Samet et al. 2007; Habert et al. 2009; Siddique and Klaus 2009; Han et al. 2012; Tironi et al. 2014; Alujas et al. 2015). Natural clays with medium to high kaolinite content and disordered structure appear as a very reactive SCM after appropriate thermal treatment (Tironi et al. 2012). The substitution of calcined clay coupled with limestone filler has received considerable attention in recent years (Scrivener 2014; Kunther et al. 2016). Antoni et al. (2012) studied blended cements made with portland cement, limestone powder, and high-purity MK. They determined that substitution of portland cement by MK coupled with limestone filler gives an excellent performance at early ages. Blended cements containing up to 45% of a 2:1 proportion of MK and limestone filler produce better mechanical properties than the corresponding ratio to plain portland cement at 7 and 28 days.

Steenberg et al. (2011) used two different pozzolans to elaborate ternary cements: (1) metakaolin produced by thermal treatment of kaolinite (premium grade) at 480°C, and (2) smectitic clay calcined at 625°C. They reported a synergetic effect in composite portland cements containing limestone filler and calcined clays for the same portland clinker content. The synergetic effect was greater for kaolinite calcined rather than for smectitic calcined clays because of the high amount of available reactive alumina. For ternary cements containing metakaolin, Vance et al. (2013) concluded that the yield stress is reduced with an increase in limestone filler content independent of the limestone particle size.

The evolution in the hydrated phases produces variations in the porosity of the system. Senhadji et al. (2014) reported that there are fundamental differences in the pore system characteristics of portland cement and blended cements elaborated with addition of silica fume and natural pozzolan. During the hydration process, the incorporation of SCMs in mortars reduced the volume of larger pores, reduced the average pore radius, and increased the volume of smaller pores. Zhang et al. (2014) determined a significant "pore-size refinement" because the initial large-size pores were divided into several small-size pores because of the progress of hydration of SCMs (granulated blast-furnace slag, low-calcium fly ash, and basic oxygen furnace slag). Akcay and Tasdemir (2015) studied cement pastes with three metakaolin replacements (8, 16, and 24%), and three water/binder ratios (0.42, 0.35, and 0.28). They determined that as a result of the pozzolanic reaction, the amount of fine pores increased but the coarser pores significantly decreased at 28 days. Perlot et al. (2013) determined that the use of metakaolin, especially

[1]Assistant Researcher, Facultad de Ingeniería, UNCPBA and Centro de Investigaciones en Física e Ingeniería del Centro de la Provincia de Buenos Aires (CIFICEN) (UNCPBA-CICPBA-CONICET), Av. del Valle 5737, B7400JWI Olavarría, Argentina.

[2]Principal Researcher, Centro de Tecnología de recursos Minerales y Cerámica (CETMIC) (UNLP-CICPBA-CONICET) (Cno. Centenario y 506), B1897ZCA Gonnet, Argentina.

[3]Professor, Facultad de Ingeniería, UNCPBA and Centro de Investigaciones en Física e Ingeniería del Centro de la Provincia de Buenos Aires (CIFICEN) (UNCPBA-CICPBA-CONICET), Av. del Valle 5737, B7400JWI Olavarría, Argentina (corresponding author). E-mail: firassar@fio.unicen.edu.ar

Note. This manuscript was submitted on May 9, 2016; approved on February 2, 2017; published online on May 5, 2017. Discussion period open until October 5, 2017; separate discussions must be submitted for individual papers. This paper is part of the ***Journal of Materials in Civil Engineering***, © ASCE, ISSN 0899-1561.

in slurry form, combined with the incorporation of limestone filler, appears particularly suitable for self-compacting concretes' manufacture, improving durability indicators such as water porosity, water absorption coefficient, and depth of carbonation.

Therefore, it is interesting to determine the variation of pore-size distribution in blended cements elaborated with kaolinitic calcined clay and limestone filler as a means to increase the knowledge of this ternary system and provide an indicator of durability. Pores with diameter smaller than 10 nm (gel pores) practically do not contribute to water permeability and they do not affect the durability of concrete, whereas pores with diameters between 10 and 1,000 nm (capillary pores) contribute to water permeability (Tobón et al. 2015). Mindess et al. (1981) established that pores with diameter range of 10–10,000 nm affect the compressive strength.

The aim of this research is to explore the interaction between the filler effect and pozzolanic effect caused by calcined clay (CC) obtained from low-grade kaolinitic clay and limestone filler (LF) as partial replacement for portland cement in binary and ternary blended cements. Tironi et al. (2015) reported the pozzolanic activity of these blended cements as assessed by the Frattini test. At 2 days, blended cements with 5% LF and 15% CC did not have pozzolanic activity; whereas blended cements with 30% CC and 30% CC + 10% LF did have a positive result. At 7 and 28 days, all blended cements containing CC showed high pozzolanic activity. In this paper, the compressive strength, hydrated phases, and pore-size distribution in selected blended cements of the system are determined to analyze the relevance of the dilution, filler, and pozzolanic effects at different hydration ages on the pore structure and mechanical properties.

Materials and Methods

Materials and Blended Cements

For this study, a portland cement (PC) and two supplementary cementing materials, namely kaolinitic calcined clay, and limestone filler, were used to formulate binary and ternary blended cements (BC).

The PC used is a normal portland cement with a Blaine fineness of 315 m^2/kg, and its Bogués potential composition is 60% C_3S, 16.4% C_2S, 3.8% C_3A, and 11.5% C_4AF by mass. For this PC, limestone filler is added as minor component (<3%).

The CC was obtained from thermal treatment of low-grade kaolinitic clay (KC) collected at a quarry operating on the surface of the Baqueró Fm, Santa Cruz province, Argentina (Dominguez et al. 2008). The mineralogical composition of kaolinite clay was 46% kaolinite, 41% quartz, and 6% illite, and the kaolinite presents a structural disorder (Tironi et al. 2014a). The thermal treatment was made at 750°C, and this temperature was selected because of the disordered structure of kaolinite in clay (Tironi et al. 2014b). The MK content in the CC was 44%.

LF was obtained from a good limestone quarry containing 93% of calcite without clay minerals and with quartz (7%) as the main impurity, and it was ground in the cement factory.

Table 1 summarizes the chemical composition and loss on ignition (LOI) for KC, LF, and PC. The chemical composition was determined by X-ray fluorescence analysis in an external laboratory [Australian Laboratory Services (ALS), Godoy Cruz, Mendoza, Argentina]. The physical characteristics, i.e., Blaine specific surface area (SS) and particle-size distributions (d_{10}, d_{50}, and d_{90}) are given in Table 2.

Fig. 1 shows the particle-size distribution (PSD) for PC, CC, and LF. PC presents a relatively narrow PSD curve with a unimodal distribution. For supplementary materials, the volume of finer particles is larger than that of PC, but they also include coarse particles. When LF and CC are incorporated, fine and coarse fractions complete the PSD of the BC. According to Zhang et al. (2014), this combination of particles sizes increases the initial packing density of blended cement paste, promoting a more efficient use of cementitious materials.

BCs were obtained replacing PC by CC and LF with different percentages in mass: 10LF, 30CC, 5LF15CC, and 10LF30CC. The CC was replaced at levels of 15 and 30% in accordance with previous results (Tironi et al. 2014a). These replacement levels are sufficient to complete the pozzolanic reaction between the MK amount in calcined clay and the calcium hydroxide provided by hydration of PC fraction. The percentage of LF incorporated is sufficient to stimulate the pozzolanic reaction (Tironi et al. 2015).

Table 1. Chemical Composition and Loss on Ignition for Used Materials

	Chemical composition (%)									
Sample	SiO_2	Al_2O_3	Fe_2O_3	CaO	MgO	SO_3	Na_2O	K_2O	TiO_2	LOI
KC	65.7	21.1	0.85	0.26	0.22	—	0.07	0.68	0.43	7.77
LF	8.7	0.8	0.5	49.1	0.5	0.2	0.18	0.25	—	39.20
PC	21.5	3.8	3.8	64.3	0.8	2.6	0.1	1.1	—	2.10

Table 2. Particle-Size Distribution and Blaine Specific Surface Area for Used Materials

	Particle-size distribution (μm)			Blaine specific surface area (m^2/kg)
Sample	d_{10}	d_{50}	d_{90}	
CC	1.37	7.13	78.9	623
LF	2.06	9.85	146.8	515
PC	2.7	19.0	63.5	315

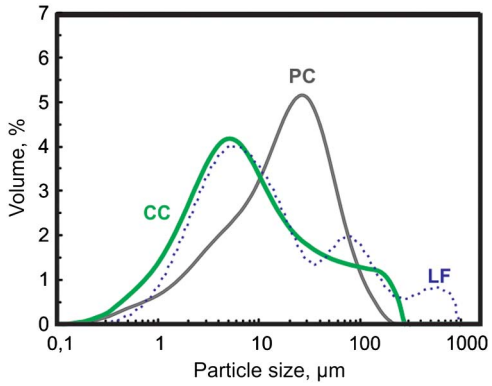

Fig. 1. Particle-size distribution for CC, LF, and PC

Compressive Strength

The mechanical performance was evaluated in terms of compressive strength at 2, 7, 28, and 90 days. Compressive strength testing was conducted on standard mortars (cement/sand = 1:3 and water/BC = 0.50) made with standard sand [EN 196-1 (BSI 2005)]. The specimens were cured in molds in a moist cabinet for 24 h and then immersed in water saturated with lime at 20 ± 1°C until the test age. The compressive strength was measured on mortar minicubes (25 × 25 × 25 mm) (Tironi et al. 2012) and the reported values correspond to the average of five specimens.

Hydration

The hydrated phases were studied in pastes prepared with w/BC of 0.50 at 2, 7, 28, 90, 180, and 360 days. At this time, fragments of paste were immersed in acetone during 24 h to stop the hydration, dried overnight in an oven at 40°C, and then cooled in a desiccator. Paste fragments were crushed and mixed with the internal crystalline standard (TiO_2) with a paste to standard ratio of 5:1 by weight. Then, it was ground in a mortar-type mill (Fritsch Pulverisette 2, Idar-Oberstein, Germany) until all mass passed through a 45-μm sieve (#325). The crystalline phases were identified by X-ray diffraction (XRD) [Philips X'Pert PW 3710 (Amsterdam, Netherlands), CuKα radiation with a graphite monochromator operating at 40 kV and 20 mA]. Later, crystalline phases and amorphous material were quantified by the Rietveld method with internal standard (Gómez-Zamorano and Escalante 2009; Snellings et al. 2014) using PANalytical's *HighScore Plus* software (Kocaba 2009).

For BC pastes at 7 days, differential thermal analysis and thermogravimetric method (DTA/TG) was carried out using a Netzch (Selb, Germany) STA 409 thermobalance. This determination was carried out in a N_2 atmosphere with a heating rate of 10°C/min up to 1200°C. The DTA curve shows an endothermic peak at 450–600°C that is characteristic of the CH dehydroxilation, and the mass loss determined by TG analysis in this range is directly proportional to the mass of CH in the paste (Tironi et al. 2014b). The correlation of CH mass obtained by TG and the results obtained by XRD and Rietveld analysis were used to check the accuracy of the Rietveld results.

Porosity

The pore-size distribution was determined in fragments of BC pastes using a mercury intrusion porosimeter (MIP) (ThermoFisher Sc PA440, Waltham, Massachusetts), for the pore-size diameters from 7.3 to 14,000 nm at 2, 7, 28, and 90 days. Small fragments with an approximate size of 5 mm were used and the maximum pressure was 400 MPa.

Results and Discussion

Compressive Strength

Fig. 2 shows the development of compressive strength (CS) for all mortars. At 2 days, the CS of 5LF15CC is comparable with that of PC; however, CS decreases in mortars with high levels of replacement. The high early CS of the 5LF15CC mortar, despite a substitution of 20% by mass of PC, is attributed to the filler effect caused by the inclusion of fine particles of CC (filling, heterogeneous nucleation of CH, and reduction of alkalis in pore solution) that stimulates the PC hydration (Bonavetti et al. 2003) and this contribution compensates the dilution effect. For 30CC and 10LF30CC, the reduction of CS can be attributed to the dilution effect exceeding the filler effect at this age. At 7 days, the highest CS is for 5LF15CC, and the contribution of calcined clay to CS is high (30CC attains 87% of PC strength) when compared with the 2-day-old specimens' performance. At 28 days, the maximum value of CS was for 30CC, showing that the pozzolanic effect is important, whereas the minimum value was for 10LF, indicating the later adverse effect on CS caused by LF (filler effects). For both ternary blended cements (5LF15CC and 10LF30CC), the CS was greater than 40 MPa at 28 days, indicating an acceptable mechanical performance accompanied by significant reduction of greenhouses gases (GHG) emission that will be computed by MPa of CS when a large replacement (40%) of portland cement is used. The same trend of the CS was observed at 90 days for BC with CC.

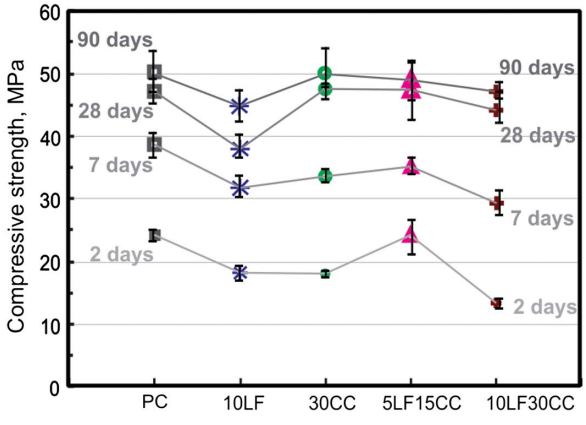

Fig. 2. Compressive strength at 2, 7, 28, and 90 days

Hydration

The XRD patterns of hydrated pastes up to 360 days are shown in Fig. 3. For PC and 10LF, the intensity of peaks assigned to CH increases up to 28 days and then remains; however, it decreases with the hydration age for blended cements containing CC. For all blended cements, the tri-substituted hydrated calcium aluminate-ferrite phases (AFt) phase (ettringite, Ett) is formed at early age, and it remains as a stable phase up to 360 days. In accordance with Kunther et al. (2016), two mono-substituted hydrated calcium aluminate-ferrite phases (AFm) phases containing carbonates were detected: hemicarboaluminate (HC) and monocarboaluminate (MC) with variable proportions over time. The peaks of HC and MC were not detected at 2 days. For PC, MC was detected at 7 days and their peaks were well defined at 90 days. For 10LF, MC was clearly identified at 28 days. For 30CC, the AFm phase was a HC–MC mixture at 7 days and then HC was detected at 28 and 90 days. Finally, the MC peaks are clearly assigned, coexisting with low-crystalline HC. According to Antoni et al. (2012), the intensity of the peak assigned to MC increased considerably after 7 days for blended cements elaborated with LF and CC (5LF15CC and 10LF30CC). From 28 days, HC was detected in the 10LF30CC paste with low intensity peaks.

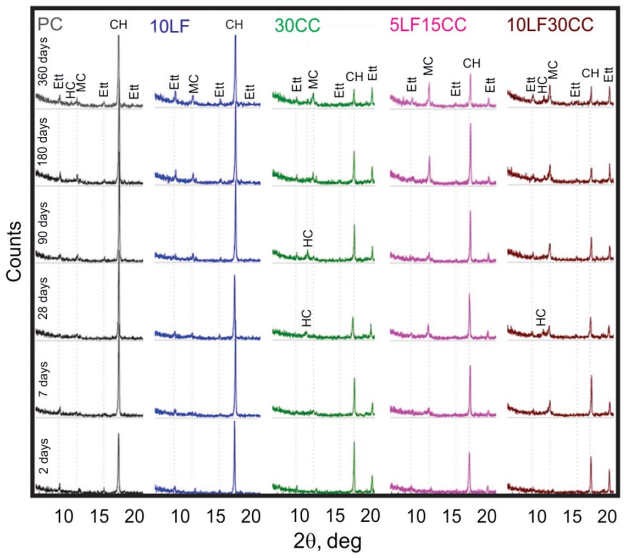

Fig. 3. XRD patterns of hydrated pastes at 2, 7, 28, 90, 180, and 360 days

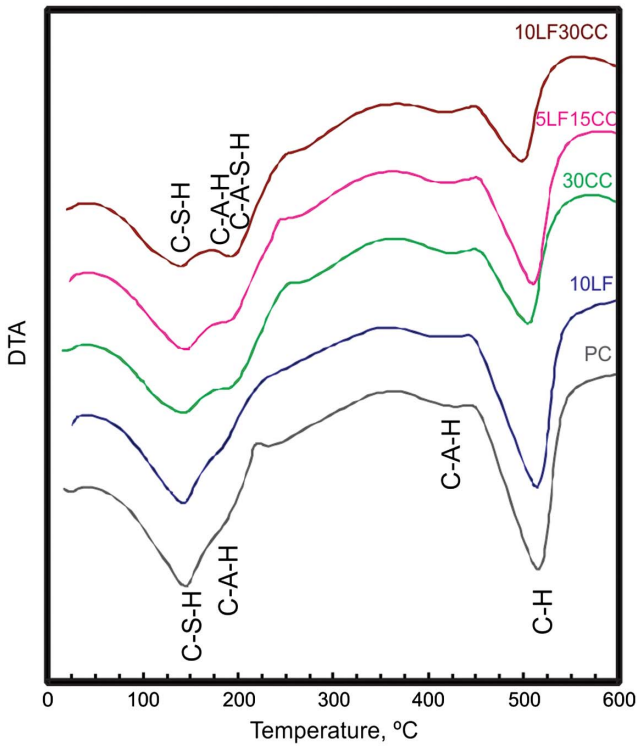

Fig. 4. DTA curves of hydrated pastes at 7 days

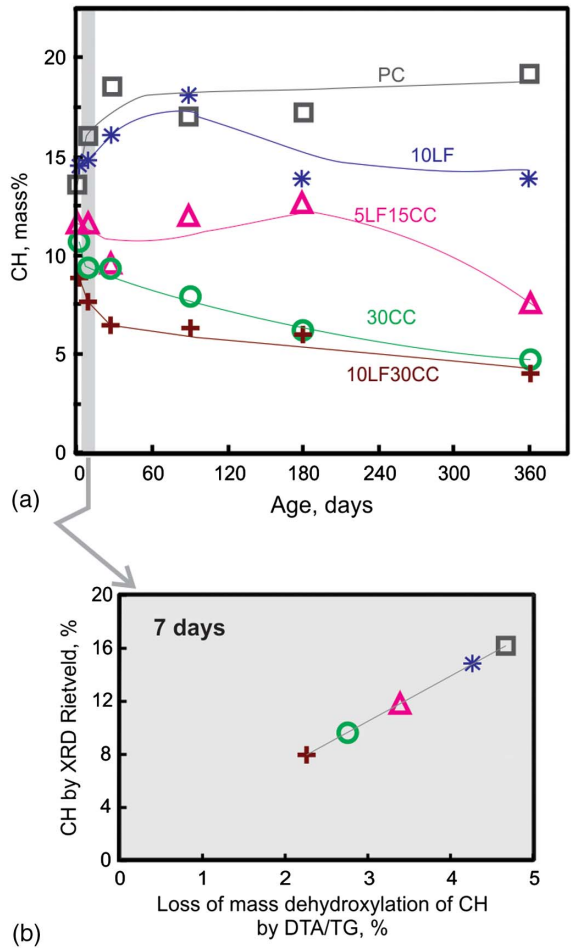

Fig. 5. Amount of CH in hydrated pastes

Fig. 4 presents the DTA analysis at 7 days. The curve of PC and 10LF shows the characteristic peaks of calcium silicate hydrate gel (C-S-H) and CH. The endothermic peak of C-S-H is centered at 145°C and the peak of aluminic phase [calcium aluminate hydrates (C-A-H)] appears as a shoulder at 190°C. The endothermic peak at 380–410°C corresponds to the decomposition of C-A-H. The reaction products formed during the pozzolanic reaction (30CC, 5LF15CC, and 10LF30CC) are C-S-H, C-A-H, and calcium aluminate silicate hydrate gel (C-A-S-H), producing an increase in the area and the intensity of the first peak (Tironi et al. 2014b). The temperature range of the CH dehydroxylation is observed at 450–575°C.

The amount of CH determined by Rietveld analysis in hydrated pastes at 2, 7, 28, 90, 180, and 360 days are shown in Fig. 5. Additionally, Fig. 5(b) shows the correlation between the mass loss determined by TG from 450 to 575°C and the CH content determined by Rietveld method at 7 days. A good correlation was obtained, indicating the accuracy of results obtained by Rietveld analysis. At 2 days, 10LF contains the greatest amount of CH because of filler effects (Bonavetti et al. 2003). For 30CC, the CH content was lower than the expected by dilution (0.70 of PC value), indicating some CH consumption because of the pozzolanic reaction with the 13.2% of MK in 30CC. For 5LF15CC, the theoretical CH-content calculated as the difference between the CH released by PC minus the dilution effect of filler particles (5% of LF and 8.4% of quartz from CC) and the amount reacted with CC in binary cement, is higher than the measured CH content. Therefore, it can be inferred that stimulation of pozzolanic reaction could occur as a result of LF addition. At 7 days, the BC pastes with CC presents lower contents of CH because of either a dilution effect or pozzolanic effect. For 30 and 40% of total replacement at 360 days, the CH content is lower than the reduction expected when computing the dilution effect: 8.5 and 7.5% for 30CC and 10LF30CC, respectively. This indicates that pastes containing 30% CC consumed more CH than those containing the same proportion of CC and 10% LF. Therefore, it can observe that LF does not contribute to the development of the pozzolanic reaction at a later age.

Fig. 6 shows the amount of AFt and AFm phases determined from quantification by XRD analysis and Rietveld method for hydrated pastes at 2, 7, 28, 90, 180, and 360 days. The Ett content in PC paste [Fig. 6(a)] remains stable (~10%) until 180 days and then it increases at 360 days. For 10LF, it is lower than the corresponding to PC and the amount decreases from 2 to 28 days, and then it increases. For BC containing CC (30CC, 5LF15CC, and 10LF30CC), the Ett content decreases from 2 to 28 days and then it increases and remains with a similar value to that determined at 2 days.

For PC, 10LF, and 30CC, the MC content increases from 7 to 90 days and then it remains at ~8.5% by mass. For 30CC, the HC phase increases up to 3% at 90 days and then it decreases. For 5LF15CC and 10LF30CC, the MC content increases continuously from 7 to 90 days and it has the highest content [Fig. 6(b)] at later ages.

For PC and 10LF, the Ett remains and increases because of a low C_3A/SO_3 ratio of the cement used that prevent monsulfoaluminate formation; the later hydration of C_4AF contributes to its formation and the presence of LF favors its stability because of the MC formation. The later hydration of C_4AF was corroborated by the reduction of the peak intensity of the brownmillerite phase at 12.2° 2θ. The formation of the products of pozzolanic reaction in blended cements with CC probably causes the reduction of available Al in the system, and the Ett content decreases until 28 days.

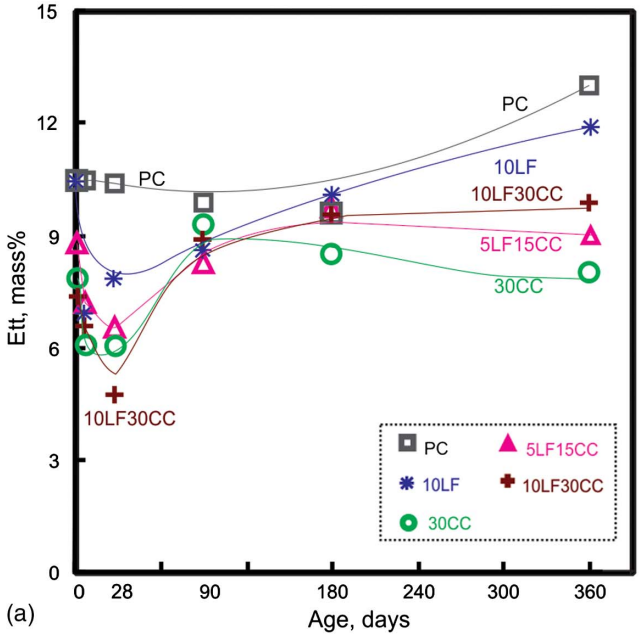

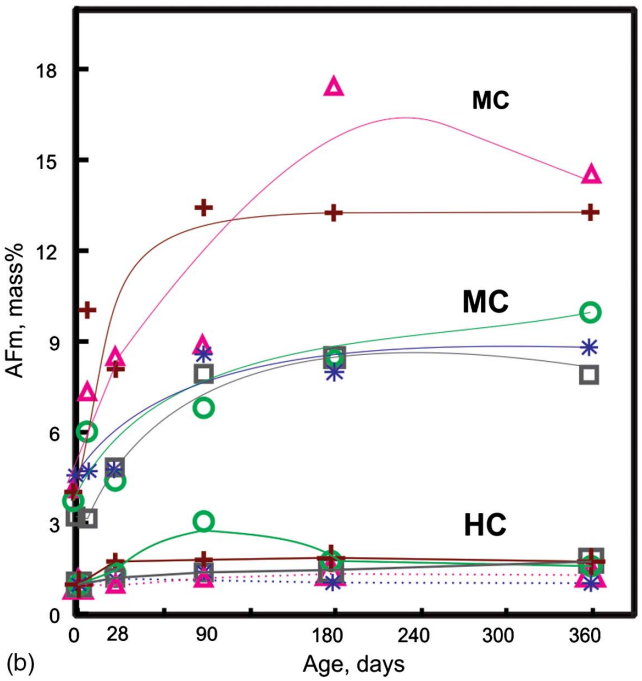

Fig. 6. Amount of (a) AFt phase Ett; (b) AFm phase HC and MC in hydrated pastes

For 30CC, the low content of Ett and MC compared with the ternary cements indicates that part of Al released by the pozzolanic reaction formed a C-A-S-H gel (Fig. 4, Alujas et al. 2015). The disposition of Al into the gel contributes to increase the compressive strength. For fly ash-limestone filler blended cements, De Weerd et al. (2011) concluded that the aluminum released by fly ash does not go only into AFm and AFt phases, but some part is also incorporated in the C–S–H gel, as observed by the increase of the Al/Si ratio into the gel.

After 90 days, 5LF15CC and 10LF30CC have the highest content of MC [Fig. 6(b)] and low content of Ett [Fig. 6(a)] in this order, indicating that LF contributes to stabilizing the Al in the phase formed in the pozzolanic reaction as MC. The high content of MC [Fig. 6(b)] and the presence of Ett [Fig. 6(b)] in ternary blended cements agree with previous results reported by Matschei et al. (2007). When LF is added, the stabilization of Ett occurs as a result of the increase in free sulfates, which are released from monosulphoaluminate (MS) when it reacts with carbonates to form HC and MC. The anion balance in the AFm phase may not change without formation/dissolution of other phases. The LF added will not react directly with portlandite or C–S–H but will react with AFm phases, including the C_4AH_x obtained from the pozzolanic reaction of MK (Lothenbach et al. 2011).

Both carbonate AFm phases are thermodynamically stable at ambient conditions in unaltered cement paste, but their thermodynamic properties are different (Matschei et al. 2007). Table 3 provides the solubility equilibrium equations and solubility products (Kps) expressed as log (Lothenbach 2010). For C_4AH_{13}, HC and MC, the values are −24.40, −29.13, and −31.47, respectively, indicating that MC is the most stable phase (minor solubility) when calcite is in excess. For MS and Ett, the log Kps is −29.26 and −44.9, respectively. Then, when free SO_4^{-2} is available, the more stable phase (Ett) is formed, the MS phase was not identified, and the amount of MC increased (Fig. 6).

Porosity

Fig. 7 shows the differential volume of mercury intrusion (dV) versus pore diameter (d) obtained from different BC pastes at 2, 7, 28, and 90 days. In these curves, two maximums (dV_{max1} and dV_{max2}), corresponding to the two most probable pore diameters (d_1 and d_2), were identified. Table 3 summarizes these values for the studied pastes from 2 to 90 days.

At 2 days [Fig. 7(a)], the pore diameter (d_1) for dV_{max1} is near to the upper limit of the capillary pores (~1,000 nm) and it drops to lower values when the hydration progresses [Figs. 7(b–d)]. The second maximum (dV_{max2}) is located in pore-size range near the lower limit of the capillary pores (~10 nm). For all pastes [Fig. 7(a)], d_1 is approximately 630 nm and the second diameter (d_2) decreases when CC or LF are added. This result is mainly attributed to the filler effect of very fine particles, which improves the initial packing and stimulates the PC hydration. The combination of LF and CC also decreases d_2 values (Table 4). PC paste has the lowest pore volume at the first maximum (dV_{max1} is the lowest) and it develops the highest compressive strength; 10LF and 30CC have a similar value of dV_{max1} and both cements attain comparable values of early strength; 10LF30CC has the greater dV_{max1} developing lower compressive strength (Table 4). The dilution effect is very important, causing increases in the effective water to cement ratio. On the contrary, 5LF15CC presents a dV_{max1} greater than the corresponding to 30CC and 10LF, but dV_{max2} occurs at a small pore diameter (d_2 in Table 4). At this age, the dilution, filler, and pozzolanic effects compete and, in accordance to their preeminent influence, affect the developed pore structure.

At 7 days [Fig. 7(b)], the d_1 of PC decreases up to 422 nm and the dV_{max1} reduced 2.5 times (from 16.5 to 6.5 mm^3/g) compared with 2 days; the dV_{max2} at 83 nm slightly increases (from 10.3 to 13 mm^3/g) because of the hydration progress (Table 4). For 10LF, the curve is wider and dV_{max1} is located at 125 nm. Blended cement with high compressive strength (5LF15CC) has low values of dV_{max1} and dV_{max2}. For 30CC and 10LF30CC, the curve shows a greater dV_{max1}, indicating that the large volume of pores is located at the same pore size ($d_1 = 84$ nm). The incorporation of CC causes an increase in pore volume with diameters smaller than 50 nm. The d_1 decreases when the replacement level increases. The developed pore structures in pastes containing CC show that the volume of large pores drops between 2 and 7 days because of

Table 3. Compounds Present in Solubility Equilibrium Equations of Hydrated Phases and Log Kps Values (Data from Lothenbach 2010)

Hydrated phases	Log Kps	Compounds presents in solubility equilibrium equations	
		Solid-state compounds	Compounds in the solution
C_4AH_{13}	−24.40	$Ca_4Al_2(OH)_{14} \cdot 6H_2O(s)$	$4Ca^{2+}(aq) + 2Al(OH)_4^-(aq) + 6OH^-(aq) + 6H_2O(l)$
HC	−29.13	$Ca_4Al_2(CO_3)_{0.5}(OH)_{13} \cdot 5.5H_2O(s)$	$4Ca^{2+}(aq) + 2Al(OH)_4^-(aq) + 0.5CO_3^{2-}(aq) + 5OH^-(aq) + 5.5H_2O(l)$
MC	−31.47	$Ca_4Al_2(CO_3)(OH)_{12} \cdot 5H_2O(s)$	$4Ca^{2+}(aq) + 2Al(OH)_4^-(aq) + CO_3^{2-}(aq) + 4OH^-(aq) + 5H_2O(l)$
MS	−29.26	$Ca_4Al_2(SO_4)(OH)_{12} \cdot 6H_2O(s)$	$4Ca^{2+}(aq) + 2Al(OH)_4^-(aq) + SO_4^{2-}(aq) + 4OH^-(aq) + 6H_2O(l)$
Ett	−44.9	$Ca_6Al_2(SO_4)_3(OH)_{12} \cdot 26H_2O(s)$	$6Ca^{2+}(aq) + 2Al(OH)_4^-(aq) + 3SO_4^{2-}(aq) + 4OH^-(aq) + 26H_2O(l)$

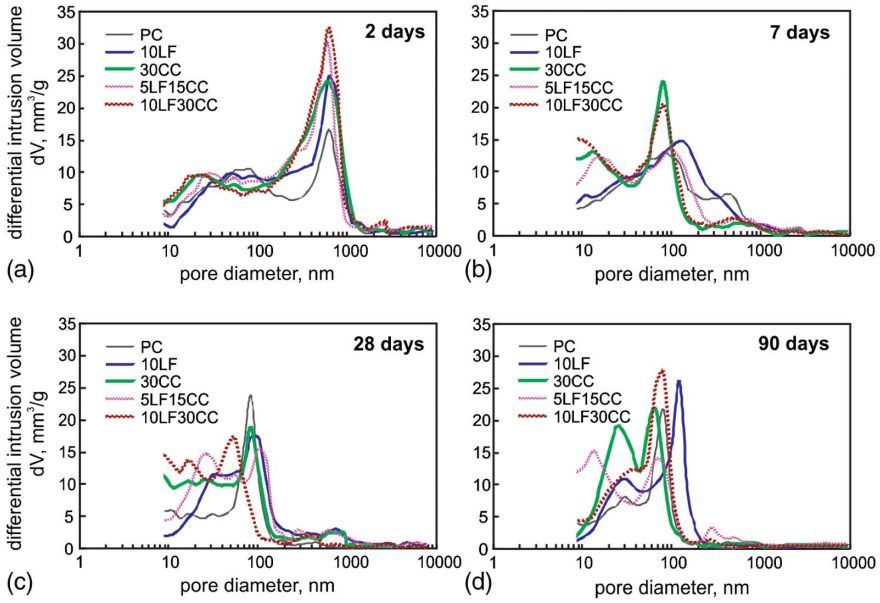

Fig. 7. Pore-size distribution in hydrated pastes at (a) 2; (b) 7; (c) 28; (d) 90 days

the filling produced by the products of pozzolanic reactions and the filler effect. At this time, the filler and pozzolanic effects are more significant and the dilution effect loses importance.

At 28 days, d_1 is lower than 100 nm for all blended cements. PC has the highest dV_{max1} and the lower volume of pores between 10 and 50 nm. For 30CC, dV_{max1} is lower than the corresponding to PC, but it has a large volume of pores between 10 and 50 nm, and high compressive strength [Fig. 7(c) and Table 4] remarking the importance of the pozzolanic effect at this age. For PC and 30CC, dV_{max2} is absent, but it is clearly identified for pastes containing LF. The distribution of pores in the ternary BC pastes is a combination of the distribution of pores in the binary pastes (10LF and 30CC).

At 90 days, the pore-size distribution for 10LF shows that the influence of LF addition is null. For binary and ternary BC with CC, the volume of pores between 10 and 50 nm increases without affecting the compressive strength [Fig. 7(d) and Table 4].

Fig. 8(a) shows the relationship between the capillary pore volume (diameter from 10 to 14,000 nm) of paste and the compressive strength of mortar. It presents an inversely exponential relationship between compressive strength and porosity. Some deviations in this relationship could be attributed to the nature of hydration products formed and the volume that they occupy reducing the pore volume but without contributing to compressive strength (Tironi et al. 2014a). Fig. 8(b) shows this relationship considering pore diameter ranging from 50 to 14,000 nm. This adjustment is also good, showing that the increase in pore volume between 10 and 50 nm caused

Table 4. Analysis of Differential Volume of Mercury Intrusion; Maximum dV_{max1} and dV_{max2} Corresponding to the Two Most Probable Pore Diameters (d_1 and d_2) at 2, 7, 28, and 90 days

Age (days)	Parameter of analysis	PC	10LF	30CC	5LF15CC	10LF30CC
2	d_1 (nm)	634	631	634	631	633
	dV_{max1} (mm^3/g)	16.5	24.8	24.0	29.7	32.4
	d_2 (nm)	68	~56	25	~20	20
	dV_{max2} (mm^3/g)	10.3	~10.6	10.6	~11.5	10.6
	CS (MPa)	24.1	18.0	18.0	23.8	13.3
7	d_1 (nm)	422	125	83	125	83
	dV_{max1} (mm^3/g)	6.5	14.7	23.9	13.5	20.4
	d_2 (nm)	83	—	13	20	~11
	dV_{max2} (mm^3/g)	13.0	—	13.2	12.3	~14.7
	CS (MPa)	38.5	31.8	33.6	35.2	29.2
28	d_1 (nm)	84	84	83	102	56
	dV_{max1} (mm^3/g)	23.8	17.2	18.7	15.5	17.0
	d_2 (nm)	—	30	—	25	16
	dV_{max2} (mm^3/g)	—	11.3	—	14.6	13.6
	CS (MPa)	47.1	38.4	48.0	47.1	44.2
90	d_1 (nm)	83	125	55	68	83
	dV_{max1} (mm^3/g)	27.2	26.1	13.7	13.8	27.2
	d_2 (nm)	—	30	25	13	~37
	dV_{max2} (mm^3/g)	—	11.5	18.9	15.1	~12.3
	CS (MPa)	50.1	44.7	49.6	48.5	47.2

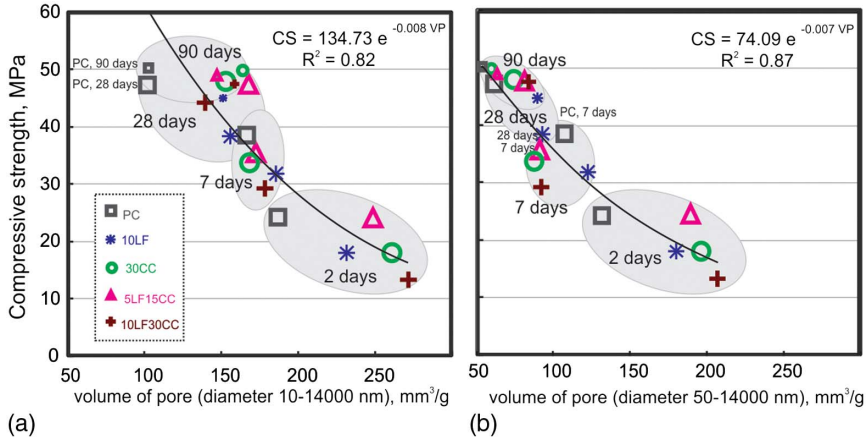

Fig. 8. Relationship between the compressive strength and volume of pores with diameters between (a) 10 and 14000 nm; (b) 50 and 14000 nm

by the addition of LF and CC does not affect the compressive strength. These results agree with the results obtained for other SCMs (Zhang et al. 2014; Akcay and Tasdemir 2015), where the amount of fine gel pores increases and those of the coarser pores significantly decreased.

Conclusions

The results of this study have indicated the effect of limestone filler and kaolinitic calcined clay (44% metakaolinite) in binary and ternary portland blended cements on the hydrated phases, pore-size distribution, and mechanical properties, and the following conclusions can be drawn. The hydrated phase's assemblage changes with the addition of LF and CC. For binary BC with CC, the increase of compressive strength at later ages is attributable to C-A-S-H formation. For ternary BC, the formation of AFt phases at an early age and the increment of MC content from 7 to 90 days also contribute to a dense microstructure.

Computing the CH content in binary and ternary cements, the addition of limestone filler is favorable to developing the pozzolanic reaction of kaolinitic calcined clay at an early age, but its contribution is not significant at later ages.

In binary and ternary BC with CC, the volume of pores ranging from 10 to 50 nm in diameter increases at later ages, but the compressive strength is unaffected. The volume of coarser pores is significantly reduced, contributing to the potential durability.

This study has shown that dilution, filler, and pozzolanic effects are relevant at 2 days, filler and pozzolanic effects are important at 7 days, and the pozzolanic effect is the most important at later ages.

Acknowledgments

The authors gratefully acknowledge the ANPCyT-FonCyT (Grant PICT-2012-0160) and Universidad Nacional del Centro de la Provincia de Buenos Aires (UNCPBA)for providing financial support for this research.

References

Akcay, B., and Tasdemir, M. (2015). "Investigation of microstructure properties and early age behavior of cementitious materials containing metakaolin." *CONCREEP 10*, C. Hellmich, B. Pichler, and J. Kollegger, eds., ASCE, Reston, VA, 1468–1475.

Alujas, A., Fernández, R., Quintana, R., Scrivener, K. L., and Martirena, F. (2015). "Pozzolanic reactivity of low grade kaolinitic clays: Influence of calcination temperature and impact of calcination products on OPC hydration." *Appl. Clay Sci.*, 108, 94–101.

Antoni, M., Roseen, J., Martirena, F., and Scrivener, K. (2012). "Cement substitution by a combination of metakaolin and limestone." *Cem. Concr. Res.*, 42(12), 1579–1589.

Bonavetti, V., Donza, H., Menéndez, G., Cabrera, O., and Irassar, E. F. (2003). "Limestone filler cement in low w/c concrete: A rational use of energy." *Cem. Concr. Res.*, 33(6), 865–871.

BSI (British Standards Institution). (2005). "Methods of testing cement. Determination of strength." *BS EN 196-1*, London.

Damtoft, J. S., Lukasik, J., Herfort, D., Sorrentino, D., and Gartner, E. M. (2008). "Sustainable development and climate change initiatives." *Cem. Concr. Res.*, 38(2), 115–127.

De Weerdt, K., Ben Haha, M., Le Saout, G., Kjellsen, K. O., Justnes, H., and Lothenbach, B. (2011). "Hydration mechanisms of ternary portland cements containing limestone powder and fly ash." *Cem. Concr. Res.*, 41(3), 279–291.

Dominguez, E., Iglesias, C., and Dondi, M. (2008). "The geology and mineralogy of a range of kaolins from the Santa Cruz and Chubut Provinces, Patagonia (Argentina)." *Appl. Clay Sci.*, 40(1–4), 124–142.

Gedam, B. A., Bhandari, N. M., and Upadhyay, A. (2015). "Influence of supplementary cementitious materials on shrinkage, creep, and durability of high-performance concrete." *J. Mater. Civ. Eng.*, 10.1061/(ASCE)MT.1943-5533.0001462, 04015173.

Gómez-Zamorano, L. Y., and Escalante, J. I. (2009). "Hydration and microstructure of portland cement partially substituted with ultrafine silica." *Mater. Constr.*, 59(296), 5–16.

Habert, G., Choupay, N., Escadeillas, G., Guillaume, D., and Montel, J. M. (2009). "Clay content of argillites: Influence on cement based mortars." *Appl. Clay Sci.*, 43(3–4), 322–330.

Han, J., Shui, Z., and Wang, G. (2012). "Research on the reactivity of metakaolin with different grade." *Sustainable Constr. Mater.*, 10.1061/9780784412671.0015, 173–180.

Hicks, J. (2010). "Durable 'green' concrete from activated pozzolan cement." *Green Streets and Highways 2010: An Interactive Conf. on the State of the Art and How to Achieve Sustainable Outcomes*, Neil Weinstein, ed., ASCE, Reston, VA, 408–430.

HighScore Plus v3.0 [Computer software]. PANalytical B.V., Almelo, Netherlands.

Juenger, M. C. G., and Siddique, R. (2015). "Recent advances in understanding the role of supplementary cementitious materials in concrete." *Cem. Concr. Res.*, 78, 71–80.

Kocaba, V. (2009). "Development and evaluation of methods to follow microstructural development of cementitious systems including slags." Ph.D. thesis, Faculté Sciences et Techniques de l'Ingénieur, École Polytechnique Fédérale de Lausanne, Ecublens, Switzerland.

Kunther, W., Dai, Z., and Skibsted, J. (2016). "Thermodynamic modeling of hydrated white portland cement-metakaolin–limestone blends utilizing hydration kinetics from 29Si MAS NMR spectroscopy." *Cem. Concr. Res.*, 86, 29–41.

Lothenbach, B. (2010). "Thermodynamic equilibrium calculations in cementitious systems?" *Mat. Struct.*, 43(10), 1413–1433.

Lothenbach, B., Scrivener, K., and Hooton, R. D. (2011). "Supplementary cementitious materials." *Cem. Concr. Res.*, 41(12), 1244–1256.

Matschei, T., Lothenbach, B., and Glasser, F. P. (2007). "The AFm phase in portland cement." *Cem. Concr. Res.*, 37(2), 118–130.

Mindess, S., and Young, J. F. (1981). *Concrete*, Prentice Hall, Upper Saddle River, NJ.

Perlot, C., Rougeau, P., and Dehaudt, S. (2013). "Slurry of metakaolin combined with limestone addition for self-compacted concrete. Application for precast industry." *Cem. Concr. Compos.*, 44, 50–57.

Potgieter-Vermaak, S., and Potgieter, J. (2006). "Metakaolin as an extender in South African cement." *J. Mater. Civ. Eng.*, 10.1061/(ASCE)0899-1561(2006)18:4(619), 619–623.

Radlinski, M., Harris, N., and Moncarz, P. (2011). "Sustainable concrete: Impacts of existing and emerging materials and technologies on the construction industry." *AEI building integration solutions*, A. C. Lynn and R. Reitherman, eds., ASCE, Reston, VA, 252–262.

Samet, B., Mnif, T., and Chaabouni, M. (2007). "Use of a kaolinitic clay as a pozzolanic material for cements: Formulation of blended cement." *Cem. Concr. Compos.*, 29(10), 741–749.

Scrivener, K. L. (2014). "Options for the future of cement." *Indian Conc. J.*, 88(7), 11–21.

Senhadji, Y., Escadeillas, G., Mouli, M., and Khelafi, H. (2014). "Influence of natural pozzolan, silica fume and limestone fine on strength, acid resistance and microstructure of mortar." *Powder Technol.*, 254, 314–323.

Shvarzman, A., Kovler, K., Grader, G. S., and Shter, G. E. (2003). "The effect of dehydroxylation/amorphization degree on pozzolanic activity of kaolinite." *Cem. Concr. Res.*, 33(3), 405–416.

Siddique, R., and Klaus, J. (2009). "Influence of metakaolin on the properties of mortar and concrete: A review." *Appl. Clay Sci.*, 43(3–4), 392–400.

Snellings, R., Salze, A., and Scrivener, K. L. (2014). "Use of X-ray diffraction to quantify amorphous supplementary cementitious materials in anhydrous and hydrated blended cements." *Cem. Concr. Res.*, 64, 89–98.

Steenberg, M., Herfort, D., Poulsen, S. L., Skibsted, J., and Damtoft, J. S. (2011). "Composite cement based on portland cement clinker, limestone and calcined clay." *Proc., 13th Int. Conf. on the Chemistry of Cement*, A. Palomo, A. Zaragoza, and J. C. López Agüí, eds., Instituto de Ciencias de la Construcción "Eduardo Torroja," Madrid, Spain.

Tironi, A., Castellano, C. C., Bonavetti, V. L., Trezza, M. A., Scian, A. N., and Irassar, E. F. (2014). "Kaolinitic calcined clays-portland cement system: Hydration and properties." *Con. Build. Mat.*, 64, 215–221.

Tironi, A., Scian, A. N., and Irassar, E. F. (2015). "Ternary blended cement with limestone filler and kaolinitic calcined clay." *Calcined clays for sustainable concrete: RILEM bookseries*, K. Scrivener and A. Favier, eds., Vol. 10, Springer, Dordrecht, Netherlands, 195–201.

Tironi, A., Trezza, M. A., Scian, A. N., and Irassar, E. F. (2012). "Kaolinitic calcined clays: Factors affecting its performance as pozzolans." *Constr. Build. Mat.*, 28(1), 276–281.

Tironi, A., Trezza, M. A., Scian, A. N., and Irassar, E. F. (2014a). "Potential use of Argentine kaolinitic clays as pozzolanic material." *Appl. Clay Sci.*, 101, 468–476.

Tironi, A., Trezza, M. A., Scian, A. N., and Irassar, E. F. (2014b). "Thermal analysis to assess pozzolanic activity of calcined kaolinitic clays." *J. Therm. Anal. Calorim.*, 116(2), 547–556.

Tobón, J. I., Payá, J., and Restrepo, O. J. (2015). "Study of durability of portland cement mortars blended with silica nanoparticles." *Constr. Build. Mat.*, 80, 92–97.

Vance, K., Kumar, A., Sant, G., and Neithalath, N. (2013). "The rheological properties of ternary binders containing portland cement, limestone, and metakaolin or fly ash." *Cem. Concr. Res.*, 52, 196–207.

Zhang, T., Liu, X., Wei, J., and Yu, Q. (2014). "Influence of preparation method on the performance of ternary blended cements." *Cem. Concr. Compos.*, 52, 18–26.